Monotonic, Cyclic, and Post-Cyclic Response of Willamette River Silt at the Van Buren Bridge

Ali Dadashiserej[1]; Amalesh Jana[2]; Susan C. Ortiz[3]; James J. Walters[4]; Armin W. Stuedlein[5]; and T. Matthew Evans[6]

[1]Graduate Student, School of Civil and Construction Engineering, Oregon State Univ., Corvallis, OR. Email: dadashia@oregonstate.edu
[2]Graduate Student, School of Civil and Construction Engineering, Oregon State Univ., Corvallis, OR. Email: janaa@oregonstate.edu
[3]Senior Geotechnical Engineer, Oregon Dept. of Transportation, Salem, OR. Email: Susan.C.ORTIZ@odot.state.or.us
[4]Senior Engineer, Shannon & Wilson, Inc., Lake Oswego, OR. Email: jjw@shanwil.com
[5]Professor, School of Civil and Construction Engineering, Oregon State Univ., Corvallis, OR. Email: armin.stuedlein@oregonstate.edu
[6]Professor, School of Civil and Construction Engineering, Oregon State Univ., Corvallis, OR. Email: matt.evans@oregonstate.edu

ABSTRACT

This study presents a laboratory investigation of the monotonic, cyclic, and post-cyclic responses of a lightly overconsolidated, low plasticity silt deposit conducted to support the geotechnical design of a proposed bridge replacement crossing the Willamette River in Corvallis, OR. The design seismic hazard corresponded to the 975-year return period with the Cascadia Subduction Zone contributing the greatest portion of the hazard. The response of the intact, natural specimens was compared to that of specimens reconstituted from the same material for comparison of the effect of soil fabric. Constant-volume cyclic stress controlled direct simple shear tests (CDSS) conducted on the low plasticity silt deposit showed cyclic mobility type behavior and increases in cyclic resistance with OCR. The exponent of the power relationship between cyclic resistance ratio (CRR) and the number of cycles, N, was shown to be smaller than that commonly assumed within the simplified method for cyclic softening of fine-grained plastic soil. Despite higher density, the reconstituted specimens exhibited approximately 16% lower cyclic resistance than their undisturbed counterparts, indicating the importance of soil fabric on the cyclic resistance of natural silt soils. The post-cyclic volumetric strain of the silt deposit was found to be independent of OCR and increased with the maximum excess pore pressure ratio generated during the cyclic tests.

INTRODUCTION

Significant damage has been attributed to earthquake-induced soil liquefaction and cyclic softening. In the last several decades, observations from case histories derived from field reconnaissance following earthquakes have helped researchers to improve the existing state of practices to anticipate future possible earthquake-induced ground failure (Bray et al. 2004, Chu et al. 2004, Cubrinovski et al. 2012, Martin et al. 2004). Numerous laboratory tests on reconstituted and intact specimens of fine-grained soils have been performed to understand their cyclic response. The importance of soil fabric on the cyclic response of transitional soil is

evident based on the cyclic test data derived from reconstituted specimens (Chang et al. 1982; Troncoso and Verdugo 1985; Koester 1994; Vaid 1994; Polito and Martin 2001) and limited comparison to natural, intact specimens (e.g., Singh 1994). Laboratory cyclic testing of natural, intact specimens continues to represent the best practice for establishing the dynamic response of transitional soils (e.g., silts) to identify the role of depositional environment, plasticity (i.e., mineralogy), fines content, and stress history on performance as demonstrated in recent efforts by Dahl et al. (2014, 2018) and Sanin and Wijewickreme (2006), Wijewickreme and Sanin (2010), and Wijewickreme et al. (2019). This study presents a laboratory investigation on the monotonic, cyclic, and post-cyclic responses of a lightly-overconsolidated, low plasticity silt deposit to support the geotechnical design of a proposed bridge replacement crossing the Willamette River in Corvallis, OR that will provide a seismically resilient crossing between Corvallis and the I-5 corridor. The east bridge approach is underlain with 3 to 4.5 m of soft to medium stiff silt. The design team was concerned cyclic softening of the silt during the life-safety controlling Cascadia Subduction Zone design event would lead to unacceptable deformations of the approach fill which would result in extensive ground improvement mitigation. The site was extensively explored with conventional mud rotary borings, suspension shear wave logging, and seismic cone penetration tests. Intact soil samples were retrieved using stainless steel Shelby tubes and conventional mud rotary techniques from two relevant soil layers. Constant-volume, stress-controlled, cyclic direct simple shear tests (CDSS) were conducted on specimens prepared from the low plasticity silt deposit and the results compared to the response of similar soil deposits with reported in the literature to identify notable differences in cyclic resistance with corresponding implications for forward predictions of seismically-induced deformations.

SOIL CHARACTERIZATION AND MONOTONIC TEST PROGRAM

Direct Simple Shear (DSS) Apparatus. The SSH-100 cyclic direct simple shear (DSS) device manufactured by Geotechnical Consulting and Testing Systems (GCTS) was used in this study. This testing system consists of hydraulically-actuated servo-controlled shear and normal load actuators and pneumatically servo-controlled cell and back pressures. Due to the general use of constant- volume testing without back-pressure saturation, which is equivalent to truly undrained condition for saturated specimens as described by Dyvik et al (1987), a pressure cell was not used in the DSS tests. The device has a fixed top cap and a sliding bottom base mounted on low-friction linear bearings. The apparatus can test cylindrical specimens with diameters of 70 mm and a typical height of 20 mm confined with a series of stacked rings (i.e., an "SGI type" DSS device) which restricts lateral deformation of the specimen during the test. The GCTS DSS apparatus used in this study is outfitted with a pair of bender element (BE) and piezoelectric disc (PD) transducers for measurements of shear wave velocity, V_s, and compression wave velocity, V_p, respectively. The V_s measurements allow for assessment of specimen quality and monitoring of changes in fabric and stiffness of the specimen subjected to shearing (e.g., Landon et al. 2007). The degree of saturation can be inferred from V_p (e.g., Stokoe and Santamarina 2000) to compare with *in-situ* conditions and gravimetric water content of the specimens.

Characterization of Silt Specimens. A laboratory testing program was conducted on intact and reconstituted specimens derived from a medium stiff silt deposit located at the project site. Intact samples were recovered from boreholes B-13 and B-14 (Table 1) using specially-fabricated Shelby tubes with a fixed piston sampler in accordance with ASTM-D1587 (ASTM

2015). Reconstituted soil samples were prepared by hydrating the crushed soil with de-aired water content twice the liquid limit for 24 hours, described as slurry deposition technique by Wijewickreme and Sanin (2010), which intends to replicate the soil fabric generated in a fluvial environment (Wijewickreme et al. 2019; Krage et al. 2020). The prepared slurry soil was consolidated under the preconsolidation pressure deduced from results of consolidation tests performed on intact specimens.

The soils evaluated are predominantly classified as low plasticity silt (ML) per the Atterberg Limits (Table 1) and the Unified Soil Classification system (USCS), and exhibit average water contents of 59% and 39% for specimens tested from boreholes B-13 (i.e., Group 1, G-1) and B-14 (i.e., Group 2, G-2), respectively. The soil samples are relatively uniform with an average plasticity index, *PI*, and fines content, *FC*, of 15 and 13, and 94% and 86%, for G-1 and G-2, respectively. In general, the specimens from both groups consist of about 73% silt-sized particles and 14% to 20% clay-sized (<0.002 mm) particles. All intact and reconstituted specimens were tested at a fully-saturated or nearly-fully saturated condition (i.e., S_r > 99.5%; Table 1) interpreted based on gravimetric water content measurements and with V_p > 700 m/s (Stokoe and Santamarina 2000, Stokoe et al. 2016). Based on the liquefaction susceptibility criterion suggested by Armstrong and Malvick (2016), the soils evaluated herein would be considered susceptible to cyclic softening, rather than liquefaction.

Table 1. Properties of the tested material from Van Buren Bridge Site.

Geographic Location of Test Site	Willamette River Corvallis, OR	
Borehole and Sample Designation (Group Number)	B-13U2 (G-1)	B-14U2 (G-2)
Sample Depth (m)	2.4 - 3.2	8.5 - 9.3
Specific Gravity, G_s	2.67	2.67
Range of Natural Water Content, w_n (%)	55 - 62	38 - 44
Average Liquid Limit, *LL*	47	40
Average Plasticity Index, *PI*	15	13
In-situ Vertical Effective Stress, $\boldsymbol{\sigma'_{v0}}$ (kPa)	50	160
Overconsolidation Ratio, *OCR*	1.8 - 2.0	1.4 - 1.7
Laboratory Shear Wave Velocity, $\boldsymbol{V_s}$ (m/s)	85 - 93	168 - 175
Laboratory Compression Wave Velocity, $\boldsymbol{V_p}$ (m/s)	NA[1]	862 - 906

[1]NA = Not available.

Representative intact specimens were trimmed to 63.4 mm × 26 mm (*D* × *H*) from intact tube samples and were subjected to constant-rate-of-strain (CRS) consolidation test without back-pressure saturation as described by Landon et al. (2018). Multiple unloading-reloading paths were conducted to determine the compression index, C_c, swelling index, C_s, and preconsolidation pressure, σ'_p, using Casagrande construction (Casagrande 1936) and work- and strain-energy based methods (Becker et al. 1987). The specimens were loaded continuously at the constant strain rate of 0.45%/h such that the measured excess pore pressure ratio, r_u, at the base of the specimens did not exceed 15% during and at the end of loading (ASTM D4186; ASTM 2012). The preconsolidation pressure estimated using Casagrande construction and the energy method varied from 90 to 100 kPa and 230 to 270 kPa for G-1 and G-2 specimens, respectively. Given the *in-situ* vertical effective stress, σ'_{v0} (Table 1), the specimens have an average overconsolidation ratio, *OCR*, of 1.9 and 1.5 for G-1 and G-2, respectively.

Specimen quality was evaluated using the work- and strain-energy based criteria proposed by DeJong et al. (2018). This framework rates the specimen quality based on the ratio of the initial recompression, $C_{ri} = \Delta e/\Delta \log \sigma'_v$, and compression indices, C_{ri}/C_c, and the ratio of strain work-based recompression index, C_{rw} $(= \Delta W/\Delta \sigma'_v)$, to strain work-based compression index, C_{rw}/C_{cw}. Specimens with compression ratios < 0.15 are classified as high quality specimens and those with compression ratio larger than 0.15 and smaller than 0.4 are rated as moderate quality (DeJong et al, 2018). The estimated index ratios indicate that the intact specimens recovered from boreholes B-13U2 and B-14U2 exhibit moderate and high quality, respectively (G-1: $C_{ri}/C_c = 0.19$; G-2: $C_{ri}/C_c = 0.12$).

Monotonic DSS Responses of Silt Specimens. Constant-volume, monotonic DSS tests were performed on intact specimens. Monotonic shear commenced after completion of primary consolidation and one log cycle of secondary compression (ASTM D6528-17; ASTM 2017) under the *in-situ* $\sigma'_{v0} = \sigma'_{vc}$ using the recompression technique. The constant-volume, shearing was performed at a strain rate of 5%/hr. Additional monotonic tests were conducted at *OCR*s of 3 and 8 to establish SHANSEP parameters (Ladd 1991) for the assessment of depth- and stress history-dependent undrained shear strengths, $s_{u,DSS}$. Figure 1 presents the results of constant-volume, monotonic, DSS tests on natural, intact and mechanically overconsolidated specimens from G-1 and G-2 specimens in terms of normalized shear stress-shear strain responses, effective stress paths, and the SHANSEP representation of the undrained shear strength defined at a shear strain, γ = 15%. The specimens exhibit a ductile stress-strain response with the typical increase in $s_{u,DSS}$ with *OCR*. Whereas the specimen with an *OCR* = 1.5 exhibits a contractive response of the entirety of undrained shearing, specimens with increasing *OCR* exhibit a transition in response that exhibit increased initial dilative tendencies prior to failure (Figure 1b). The SHANSEP parameters for these specimens (Figure 1c; S = 0.25, and m = 0.81) are in the range of reported values for the silt deposits with similar properties (Ladd 1991, Dahl et al. 2014, Jana and Stuedlein 2021).

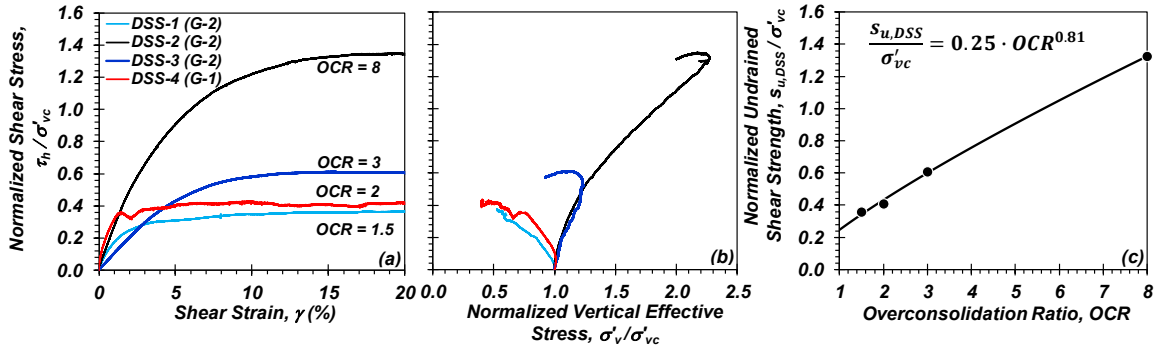

Figure 1. Monotonic undrained DSS response of intact specimens of silt: (a) normalized shear stress-shear strain responses, (b) effective stress paths, and (c) SHANSEP representation of undrained shear strength.

CYCLIC DSS TEST PROCEDURES, RESULTS, AND DISCUSSION

Cyclic DSS Test Procedures. Constant-volume, stress-controlled, cyclic direct simple shear (CDSS) tests were conducted on intact and reconstituted specimens. Specimens were consolidated under estimated *in-situ* σ'_{v0}; following completion of the consolidation and

secondary compression phases, and measurements of body wave velocities, specimens were subjected to uniform sinusoidal horizontal shear stress cycles with a specified cyclic stress ratio, $CSR = \tau_{cyc}/\sigma'_{v0}$, and loading frequency of 0.1 Hz until reaching sufficiently large single-amplitude shear strain criteria (e.g., γ_{SA} = 3%, 3.75%). Following the completion of the cyclic phase some specimens were re-centered and reconsolidated to σ'_{v0} to observe the post-cyclic volumetric strain due to the dissipation of excess pore pressure.

Cyclic Response of Intact Specimens. The fully-saturated specimen properties, test parameters, and key results for the constant-volume, stress-controlled cyclic tests on intact and reconstituted specimens are summarized in Table 2. Figure 2 compares the cyclic response of intact G-2 specimens subjected to CSRs varying from 0.22 to 0.29 in terms of normalized shear stress-shear strain, CSR-γ, hysteresis, effective stress path, accumulation of γ with number of loading cycles, N, normalized by N necessary to reach γ = 3%, $N_{\gamma=3\%}$, and excess pore pressure ratio, r_u, versus $N/N_{\gamma=3\%}$. Specimen VB-U9 was subjected to CSR = 0.22 which resulted in γ_{SA} = 3 and 3.75% after 28.2 and 34.2 cycles, respectively (Table 2 and Figure 2a). The development of excess pore pressure is interpreted as migration of σ'_v towards the origin (Figure 2b), which is about 15% in the first cycle, with a maximum of 97% after N = 53. Note that N can exceed 400 from subduction zone ground motions for soils exhibiting shallow CRR-N curves (e.g., with power law exponent, b = 0.07), such as plastic silts (Boulanger and Idriss 2015), where the equivalent N is calculated using $0.65\tau_{cyc}/\sigma'_{v0}$.

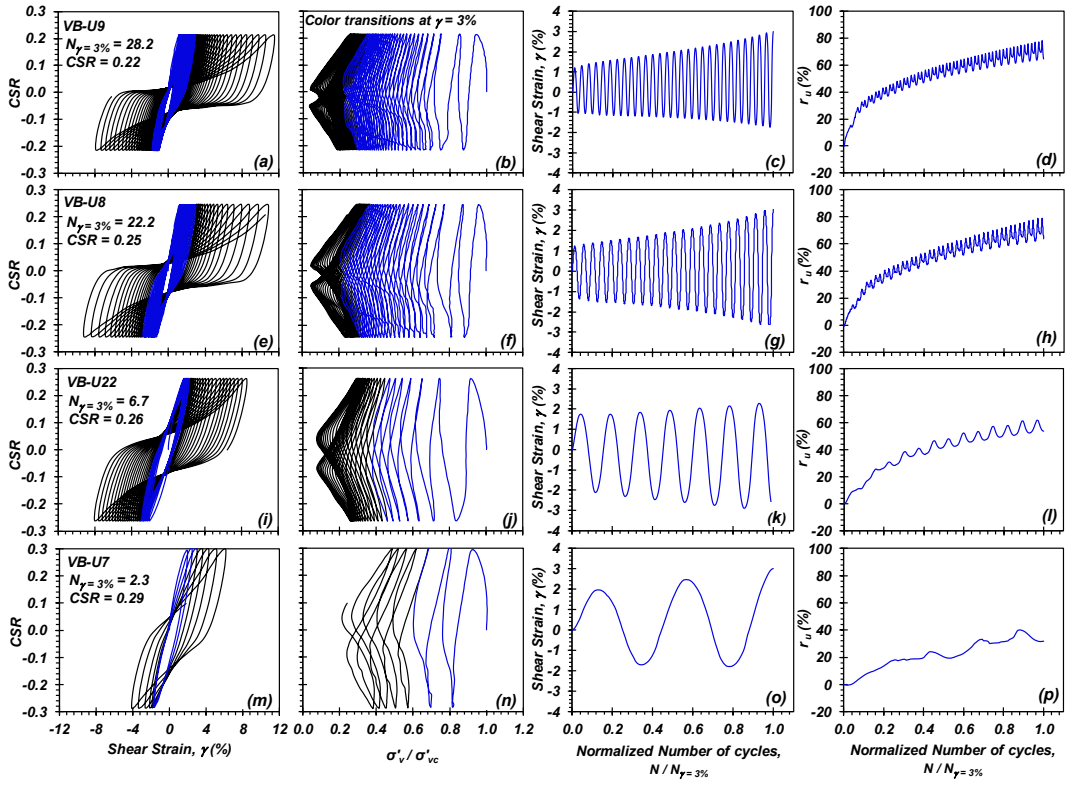

Figure 2. Comparison of cyclic response of intact specimens (Borehole B-14) indicating: (a, e, i, m) cyclic shear stress - shear strain hysteresis, (b, f, j, n) effective stress paths, (c, g, k, o) accumulation of shear strain, and (d, h, l, p) generation of excess pore pressure with normalized number of cycles, $N/N_{\gamma=3\%}$.

Table 2. Synthesis of constant-volume, stress-controlled cyclic test results.

Test ID	*In-situ* Vertical Effective Stress σ'_{v0} (kPa)	*OCR*	Plasticity Index *PI*	Fines Content *FC* (%)	Maximum Generated Excess Pore Pressure Ratio $r_{u,max}$ (%)	Cyclic Stress Ratio *CSR*	Pre-shear Void Ratio e_c	*N* γ = 3%	*N* γ = 3.75%
Intact, Natural Specimens									
				B-13U2 (G-1)					
VB-U5	50	2.0	13	95	52	0.21	1.24	720[1]	720[1]
VB-U15	50	2.0	16	91	92	0.44	1.35	2.3	4.2
VB-U18	50	2.0	16	93	82	0.38	1.38	5.3	8.2
VB-19	50	2.0	15	92	86	0.33	1.35	7.2	11.3
VB-U20	48	2.0	15	NA[2]	88	0.31	1.47	49.3	65.3
VB-U21	50	1.9	NA	NA	92	0.33	1.50	17.8	24.8
				B-14U2 (G-2)					
VB-U3	160	1.5	14	NA	48	0.14	0.97	720[1]	720[1]
VB-U7	160	1.5	13	86	79	0.29	0.95	2.3	4.2
VB-U8	160	1.5	14	81	96	0.25	0.92	22.2	26.2
VB-U9	160	1.5	11	80	97	0.22	0.90	28.2	34.2
VB-U14	160	1.5	15	99	88	0.27	0.98	1.8	3.2
VB-U17	160	1.5	13	NA	80	0.27	1.00	2.3	4.2
VB-U22	160	1.5	NA	98	92	0.26	0.89	6.8	10.7
Reconstituted Specimens									
				B-14U2 (G-2)					
VB-R1	160	1.4	12	95	91	0.22	0.84	7.2	9.3
VB-R2	160	1.5	12	NA	91	0.20	0.81	18.2	20.3
VB-R3	160	1.5	16	98	94	0.18	0.87	34.3	39.2
VB-R4	160	1.5	16	NA	88	0.22	0.84	7.7	9.7
VB-R5	160	1.5	NA	NA	77	0.25	0.85	1.2	1.8

[1] Pre-defined γ for the stated N not obtained.
[2] Not available.

The effective stress path (Figure 2b) exhibits the cyclic mobility type behavior with an initial contractive tendency followed by alternating dilation and contraction in loading and unloading, respectively (Castro and Poulos 1977; Boulanger et al. 1998; Sanin and Wijewickreme 2006; Jana and Stuedlein 2021). The cyclic mobility behavior is interpreted as an incremental accumulation of shear strain (Figure 2c), excess pore pressure generation, and degradation of shear stiffness with transient, near-zero stiffness (Figure 2a) without an abrupt loss of strength during cyclic shearing. The specimen produced narrow, inverted *s*-shaped hysteresis loops which are similar in response as dense sands (Wijewickreme et al. 2005) and non-plastic and low plasticity silts (Dahl et al. 2014; Price et al. 2017). All of the specimens presented in Fig. 2 exhibited the cyclic mobility type response which were most pronounced in those specimens subjected to lower CSRs (Figure 2a and 2e) due to the lower strain rate associated with the constant frequency of loading relative to higher CSRs, which resulted in a greater reduction in shear modulus (Vardanega and Bolton 2013). Comparison of the shear strain response of specimen VB-U9 (CSR = 0.22; Figure 2c) to specimen VB-U7 (CSR = 0.29; Figure 2o) indicates that as the CSR increases, the rate of accumulation of γ with N, and the magnitude of γ developed in first loading cycle, increase. Although subtle differences in *FC* and e_c exist between the specimens (Table 2), the lower rate of accumulation of γ in specimen VB-U9 mainly stems from

the application of a smaller CSR. Figures 2d, 2h, 2l, and 2p illustrate that for a given $N/N_{\gamma=3\%}$= 1, the maximum excess pore pressure ratio, $r_{u,max}$, decreases with increasing CSR. For example, specimen VB-U9 produced $r_{u,max}$ = 78% ($N_{\gamma=3\%}$ = 28.2; Figure 2d) compared to $r_{u,max}$ = 39% generated by specimen VB-U7 after experiencing $N_{\gamma=3\%}$= 2.3 (Figure 2p). This is due to the fact that the generation of excess pore pressure during cyclic loading is a function of N and the maximum cyclic shear strain, γ_{max} (Dahl et al. 2014; Jana and Stuedlein 2021). Therefore, specimens subjected to smaller CSRs (e.g., specimen VB-U9) require greater N and excess pore pressures to achieve a given cyclic failure criterion (e.g., γ = 3%).

Effect of Soil Fabric on Cyclic Response. Figure 3 compares the cyclic response of intact (VB-U9) and reconstituted specimens (VB-R1) subjected to identical CSR = 0.22 in terms of CSR-γ, effective stress path, and accumulation of γ and r_u with N. Similar to the intact specimens, reconstituted specimen exhibited the cyclic mobility type behavior with transient zero shear stiffness during hysteresis (Figure 3a). There are significant differences between the cyclic response of intact and reconstituted specimens. For example, both specimens exhibit contractive behavior during N = 1, transitioning to alternating dilation (loading) and contraction (unloading) as N increases (Figure 3b). However, the reconstituted specimen exhibits a greater rate of shear modulus degradation (Figure 3a), accumulation of shear strain (Figure 3c), and generation of excess pore pressure (Figure 3d), in agreement with observations reported by Sanin and Wijewickreme (2011) and Jana and Stuedlein (2021). The relative contribution of a higher density (e_c = 0.84) to the cyclic resistance of the reconstituted specimen (V_s = 159 m/s) appears significantly smaller than that of age and the corresponding soil fabric, as observed through comparison to the cyclic resistance of the less dense, intact specimen (e_c = 0.90, V_s = 168 m/s).

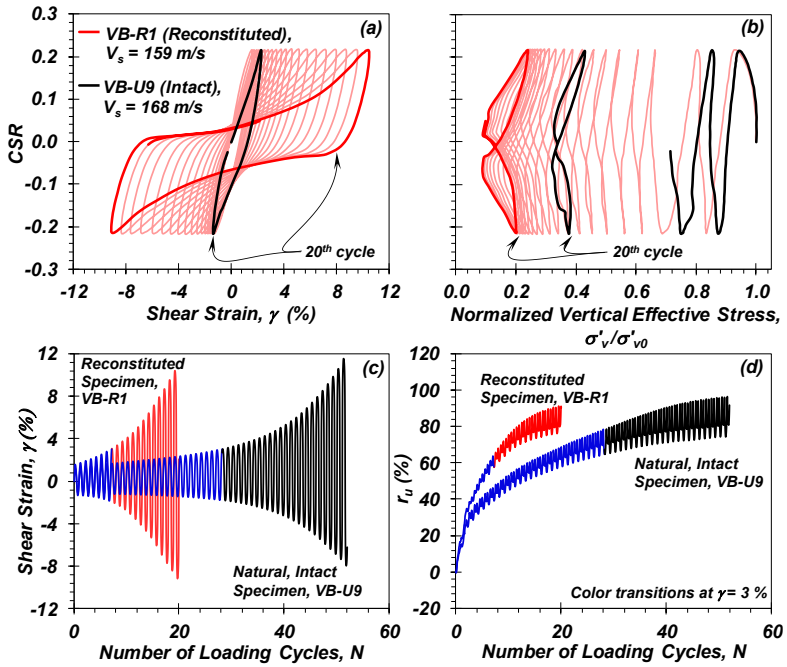

Figure 3. Comparison of intact and reconstituted specimens VB-U9 and VB-R1 (Borehole B-14): (a) cyclic shear stress - shear strain hysteresis, (b) effective stress paths, (c) accumulation of shear strain and (d) generation of excess pore pressure with normalized number of cycles, $N/N_{\gamma=3\%}$.

Cyclic Resistance of Intact and Reconstituted Specimens. Figure 4a presents the variation of the cyclic resistance ratio, CRR, with N required to reach γ_{SA} = 3% (i.e., the CRR-$N_{\gamma=3\%}$ curve) for the constant-volume, stress-controlled cyclic tests on natural intact and reconstituted specimens. A power law $CRR = a \cdot N_{\gamma}^{-b}$, where a and b represent the fitting parameters, facilitates comparison of the cyclic resistance among the various soils. The fitting parameters have been determined using ordinary least square regression equal to a = 0.452 and b = 0.106 for the intact G-1, a = 0.297 and b = 0.079 for intact G-2, and a = 0.258 and b = 0.094 for the reconstituted specimens. The exponents b are smaller than the assumed b = 0.135 for use within the simplified method for cyclic softening assessment of fine-grained plastic soils (Idriss and Boulanger 2008). Thus, both the equivalent number of loading cycles, N_{eq}, calculated using $0.65\tau_{cyc}/\sigma'_{v0}$ and the magnitude scaling factor associated with the plastic silts examined in this study would be larger than that proposed by Idriss and Boulanger (2008) for mega-thrust earthquakes based on the variation of each with b reported by Boulanger and Idriss (2015). In particular, N_{eq} for a M_w = 9^+ Cascadia Subduction Zone scenario earthquake would likely be larger than 100, given that an average N_{eq} = 70 corresponds to M_w = 7.5 for b = 0.1 (Boulanger and Idriss 2015); work is currently ongoing to clarify this design concern. Although the N_{eq} for plastic silts may be large, the corresponding CRR is less sensitive to N compared to non-plastic soils due to their shallow CRR-N curves.

Comparison of the cyclic resistance of intact specimens in Figure 4a indicates that for a given N, an increase in OCR results in an increase in CRR. For the case of $N_{\gamma=3\%}$ = 2.3, an increase in OCR from ~1.5 (G-2 specimens) to ~1.9 (G-1 specimens) results in an increase in CRR from 0.29 to 0.44. However, as σ'_{v0} = 50 kPa and 160 kPa for G-1 and G-2 specimens, respectively, differences in stress-dilatancy at these stresses contributes to the higher CRR of G-1 specimens. For the intact specimens, with N = 30, τ_{cyc}/σ'_{v0} ranges from 0.23 (G-2) to 0.32 (G-1) for OCRs ranging from 1.4 to 1.7 and 1.8 to 2.0, respectively. Figure 4a compares the cyclic response of the natural silt in the current study to other soils with comparable PIs and OCRs; the cyclic resistance of G-1 specimens (PI = 13 to 16 and OCR = 1.8 to 2.0) is similar to specimens with average PI of 18 and OCR = 2 reported by Dahl et al. (2014). Furthermore, the cyclic resistance of intact specimens from the Port of Portland reported by Jana and Stuedlein (2021), which exhibit an average PI of 28 and OCR of 1.6 to 2.2 results in 32% higher CRR compared to G-2 specimens with PI = 11 to 15 and OCR = 1.4 to 1.7, which is attributed to the higher PI for the specimens reported by Jana and Stuedlein (2021).

The comparison of the cyclic resistance of G-1 intact (average e_c = 0.94) and reconstituted specimens (average e_c = 0.84) indicate that for OCR = 1.5 and PI = 11 to 15, the intact specimens exhibited 15 to 21% higher resistance compared to the reconstituted specimens for the range of N evaluated (i.e., $1 < N < 29$), despite the higher e. This observation implies that the commonly used state variables (i.e., e_c and σ'_{v0}) may not sufficiently explain the observed differences in behavior of undisturbed and reconstituted specimens (Sanin and Wijewickreme 2011), which exhibit identical mineralogy and grain size distributions. The observed differences may be attributed to the difference in depositional environment and aging effects noted previously, resulting in differences in soil fabric. This hypothesis is confirmed by the higher V_s = 168 m/s (and maximum shear modulus, G_{max} = 52.1 MPa), of the intact specimens compared to their reconstituted counterparts (V_s = 159 m/s and G_{max} = 48.6 MPa).

Figure 4b presents the variation of cyclic strength ratio, $\tau_{cyc}/s_{u,DSS}$, with N at γ = 3% for the G-1 and G-2 specimens. The strength ratios have been adjusted to a loading frequency of 1 Hz

by considering a 9% increase in strength per log cycle of loading rate for improved representation of the response to predominant earthquake ground motion frequencies to reflect well-known strain rate-effects on undrained shear strength (e.g., Lefebvre and Lebouef 1987, Zergoun and Vaid 1994, Lefebvre and Pfendler 1996, Sheahan et al. 1996, Boulanger et al. 1998). The $\tau_{cyc}/s_{u,DSS}$ of G-1 specimens is 19 to 30% larger than the G-2 specimens (for $1 < N < 29$) consistent with the *CRR*- *N* curves in Figure 4a. Figure 4b compares the variation of $\tau_{cyc}/s_{u,DSS}$ for specimens evaluated in this study with results reported by Jana and Stuedlein (2021; *PI* = 28, *OCR* = 1.6 to 2.2) and Dahl et al. 2014 (average *PI* = 18, *OCR* = 1 and 2). The $\tau_{cyc}/s_{u,DSS}$ of G-2 specimens is similar to that of natural intact specimens reported by Dahl et al. (2014), however, they both exhibit larger strength compared to that of specimens with average *PI* of 28 and *OCR* of 1.6 to 2.2 (Jana and Stuedlein 2021). The observed differences can be attributed to the differences in soil fabric, e_c, effects of stress dilatancy, and difficulty of defining $s_{u,DSS}$ for those specimens which exhibit strain hardening during monotonic shearing (Dahl et al. 2014).

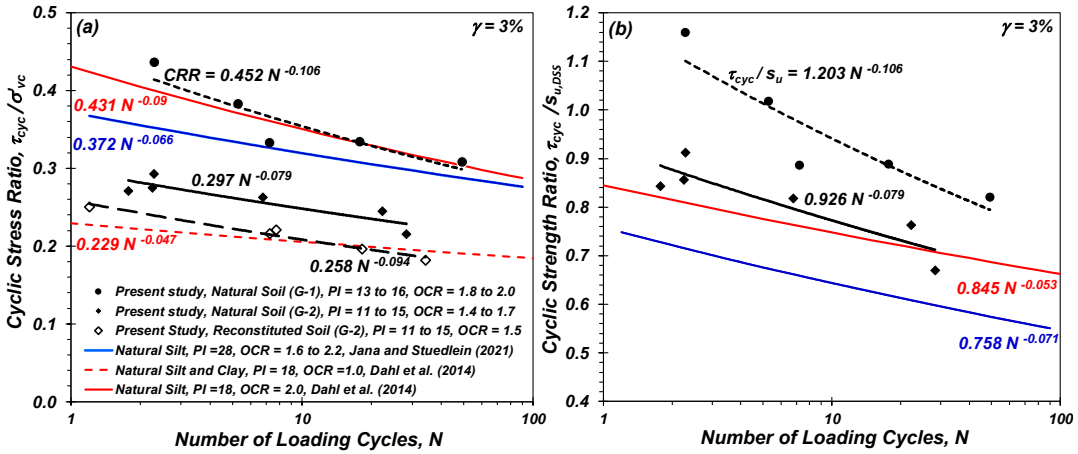

Figure 4. Comparison of cyclic resistance of intact specimens from G-1, and intact and re-constituted specimens from G-2: variation of (a) *CRR* with *N*, and (b) $\tau_{cyc}/s_{u,DSS}$ with *N* for $\gamma = 3\%$.

Post-Cyclic Reconsolidation Strain of Natural, Intact and Reconstituted Specimens. After completion of the cyclic loading phase, selected G-1 and G-2 specimens were re-centered and reconsolidated under σ'_{v0} to obtain the post-cyclic volumetric strain, ε_v, associated with different $r_{u,max}$ and γ_{max} during cyclic loading. Figure 5a presents the variation of ε_v with $r_{u,max}$ for intact and reconstituted silt specimens, indicating an increasing trend in ε_v with $r_{u,max}$. For a given $r_{u,max}$, the reconstituted specimens experienced greater ε_v compared to the intact specimens, attributed to the difference in the soil compressibility as a result of their differences in soil fabric (Wijewickreme et al. 2019; Jana and Stuedlein 2021). The variation of ε_v with $r_{u,max}$ evaluated in this study is independent of stress history and similar to the results of previous studies (Wijewickreme et al. 2019; Jana and Stuedlein 2021). The ε_v reported by Verma (2019) for a highly-plastic, structured clay (*PI* = 37) fall outside of the boundary reported by Wijewickreme et al. (2019), indicating that in addition to $r_{u,max}$, the plasticity contributes to the post-cyclic volumetric response of natural silt.

Figure 5b presents the variation of the ε_v with γ_{max} for the previously-discussed specimens. For a given *OCR* and *PI,* the reconstituted specimens experienced greater ε_v compared to the intact specimens due to greater γ_{max} generated in the cyclic loading phase. The development of ε_v depends on the magnitude of $r_{u,max}$ and γ_{max}, as compressibility varies with the degree of the soil fabric destruction during the cyclic phase (Dahl et al. 2014). The data in Figure 5b indicates that ε_v increases somewhat linearly with γ_{max}, however, a statistical model would require additional tests on intact specimens with □ ranging from 1 to 5% to confirm whether or not the apparent trend holds for both intact and reconstituted specimens.

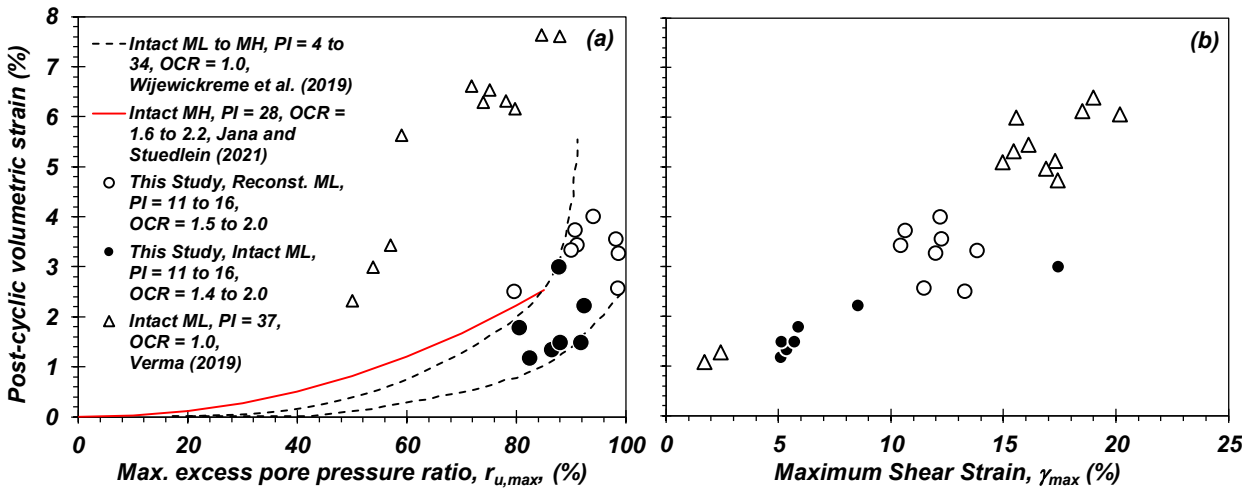

Figure 5. Comparison of post-cyclic reconsolidation responses to those previously reported: variation of volumetric strain with (a) $r_{u,max}$ and (b) γ_{max}.

CONCLUSIONS

This study presents a systematic laboratory investigation of the monotonic, cyclic, and post-cyclic responses of a low plasticity, lightly over-consolidated silt deposit. The role of governing factors such as soil fabric and stress history on the cyclic and post-cyclic response have been identified and compared to previously-reported tests to identify similarities and pertinent differences in their responses. The following may be concluded from this study:

1. The monotonic DSS responses indicates a ductile shear stress-shear strain response with increases in $s_{u,DSS}$ with *OCR*. The $s_{u,DSS}/\sigma'_{v0}$ ranges from 0.36 to 0.41 for *OCR* of 1.5 to 2.0, similar to soils with comparable *PI* reported by Dahl et al. (2018).
2. The cyclic response of the intact specimens exhibited cyclic mobility type behavior without a sudden loss of strength during cyclic shearing. Higher cyclic resistance of the G-1 specimens is associated with lower confining pressure (50 kPa) and higher *OCR* compared to G-2.
3. There are significant differences in cyclic response between intact and reconstituted specimens where reconstituted specimen exhibit higher net contractive behavior which leads to greater rate of accumulation of shear strain and excess pore pressure generation. The differences may be attributed to the difference in depositional environment, soil fabric, and aging effects which resulted in different particle structure, confirmed by shear wave velocity measurements.

4. The estimated b exponent values for the power law model for plastic silt are smaller than that commonly assumed (i.e., 0.135) for plastic silts and clays within simplified method for cyclic softening of fine-grained plastic soils proposed by Idriss and Boulanger (2008). This suggests that the number of equivalent cycles and magnitude scaling factors used with the simplified method for cyclic softening should be re-assessed to consider other soil characteristics.
5. For a given $r_{u,max}$, reconstituted specimens experience a greater post-cyclic volumetric strain, ε_v, compared to that of intact specimens due to differences in soil fabric. The variation of ε_v with $r_{u,max}$ response is independent of soil stress history, *OCR*, for the range considered, and may depend on other factors.

ACKNOWLEDGEMENTS

The university-based authors were supported in part by the National Science Foundation under grant CMMI-1663654 over the course of this investigation. Any opinions, findings, and conclusions or recommendations expressed are those of the authors and do not necessarily reflect the views of the National Science Foundation.

REFERENCES

Armstrong, R. J., and Malvick, E. J. (2016). "Practical Considerations in the use of liquefaction susceptibility criteria." *Earthquake Spectra*, 32(3), 1941-1950.

ASTM-D1587. (2015). *Standard practice for thin-walled tube sampling of fine-grained soils for geotechnical purposes*. West Conshohocken, PA: ASTM.

ASTM-D-4186. (2012). *Standard Test Method for One-dimensional Consolidation Properties of Saturated Cohesive Soils Using Controlled-strain Loading*. West Conshohocken, PA: ASTM.

ASTM D6528-17. (2017). *Standard Test Method for Consolidated Undrained Direct Simple Shear Testing of Fine Grain Soils*. West Conshohocken, PA: ASTM.

Becker, D., Crooks, J., Been, K., and Jefferies, M. (1987). "Work as a criterion for determining in situ and yield stresses in clays." *Can. Geot. J.*, 24(4), 549-564.

Boulanger, R. W., Meyers, M. W., Mejia, L. H., and Idriss, I. M. (1998). "Behavior of a fine-grained soil during the Loma Prieta earthquake." *Can. Geot. J.*, 35(1), 146-158.

Boulanger, R. W., and Idriss, I. M. (2006). "Liquefaction susceptibility criteria for silts and clays." *J. Geot. Geoenv. Eng.*, (11), 1413-1426.

Boulanger, R. W., and Idriss, I. M. (2014). "CPT and SPT based liquefaction triggering procedures." Report No. UCD/CGM.-14, 1-134, Univ. of California Davis, CA.

Boulanger, R. W., and Idriss, I. M. (2015). "Magnitude scaling factors in liquefaction triggering procedures." *Soil Dyn. Earthq. Eng.*, 79, 296-303.

Bray, J. D., Sancio, R. B., Durgunoglu, T., Onalp, A., Youd, T. L., Stewart, J. P., Seed, R. B., Cetin, O. K., Bol, E., Baturay, M. B., and Christensen, C. (2004). "Subsurface characterization at ground failure sites in Adapazari, Turkey." *J. Geot. Geoenv. Eng.*, 130(7), 673-685.

Bray, J. D., and Sancio, R. B. (2006). "Assessment of the liquefaction susceptibility of fine-grained soils." *J. Geot. Geoenv. Eng.*, 132(9), 1165-1177.

Casagrande, A. (1936). "The determination of pre-consolidation load and it's practical significance." *Proc. Int. Conf. Soil Mech. Found. Eng.* Cambridge, Mass., 1936, 60.
Castro, G., and Poulos, S. J. (1977). "Factors affecting liquefaction and cyclic mobility." *J. Geot. Geoenv. Eng.*, 103(6).
Chang, N. Y., Yeh, S. T., and Kaufman, L. P. (1982). "Liquefaction potential of clean and silty sands." *Proc., 3rd Int. Earthquake microzonation conf.*, Vol. 2, 1017-1032.
Chu, D. B., Stewart, J. P., Lee, S., Tsai, J. S., Lin, P. S., Chu, B. L., Seed, R. B., Hsu, S. C., Yu, M. S., and Wang, M. C. (2004). "Documentation of soil conditions at liquefaction and non-liquefaction sites from 1999 Chi–Chi (Taiwan) earthquake." *Soil Dyn. Earthq. Eng.*, 24, 647-657.
Cubrinovski, M., Henderson, D., and Bradley, B. A. (2012). "Liquefaction impacts in residential areas in the 2010-2011 Christchurch earthquakes." *Proc., Int. Symp. on Engineering Lessons Learned from the 2011 Great East Japan Earthquake*, Japan Association for Earthquake Engineering, Tokyo, 811–824.
Dahl, K. R., DeJong, J. T., Boulanger, R. W., Pyke, R., and Wahl, D. (2014). "Characterization of an alluvial silt and clay deposit for monotonic, cyclic, and post-cyclic behavior." *Can. Geot. J.*, 51(4), 432-440.
Dahl, K., Boulanger, R. W., and DeJong, J. T. (2018). "Trends in experimental data of intermediate soils for evaluating dynamic strength." *Proc., 11th US Nat. Conf. on Earthq. Eng.* Earthquake Engineering Research Institute.
DeJong, J. T., Krage, C. P., Albin, B. M., and DeGroot, D. J. (2018). "Work-based framework for sample quality evaluation of low plasticity soils." *J. Geot. Geoenv. Eng.*, 144(10), 04018074.
Dyvik, R., Lacasse, S., Berre, T., and Raadim, B. (1987). "Comparison of truly undrained and constant volume direct simple shear tests." *Géotechnique*, 37(1), 3-10.
Jana, A., and Stuedlein, A. W. (2021). "Monotonic, Cyclic and Post-Cyclic Response of an Alluvial Plastic Silt Deposit." *J. Geot. Geoenv. Eng.*, 147(3): 04020174.
Krage, C. P., Price, A. B., Lukas, W. G., DeJong, J. T., DeGroot, D. J., and Boulanger, R. W. (2020). "Slurry Deposition Method of Low-Plasticity Intermediate Soils for Laboratory Element Testing." *Geot. Test. J.*, 43(5), 1269-1285.
Koester, J. P. (1994). "The influence of fines type and content on cyclic strength". *Ground Failures Under Seismic Conditions*, Geotech. Spec. Publ. 44, ASCE, New York, 17–33.
Landon, M. M., DeGroot, D. J., and Sheahan, T. C. (2007). "Nondestructive sample quality assessment of a soft clay using shear wave velocity." *J. Geot. Geoenv. Eng.*, 133(4), 424-432.
Martin, J. R., Olgun, C. G., Mitchell, J. K., and Durgunoglu, H. T. (2004). "High-modulus columns for liquefaction mitigation." *J. Geot. Geoenv. Eng.*, 130(6), 561-571.
Polito, C. P., and Martin, J. R., II. (2001). "Effects of nonplastic fines on the liquefaction resistance of sands." *J. Geot. Geoenv. Eng.*, 127(5), 408-415.
Price, A., DeJong, J., and Boulanger, R. (2017). "Cyclic loading response of silt with multiple loading events." *J. Geot. Geoenv. Eng.*, 143(10), 04017080.
Sanin, M., and Wijewickreme, D. (2006). "Cyclic shear response of channel-fill Fraser River Delta silt." *Soil Dyn. and Earthq. Eng.*, 26(9), 854-869.
Sanin, M. V., and Wijewickreme, D. (2011). "Cyclic shear response of undisturbed and reconstituted Fraser River Silt." *Proc., Pan-Am CGS Geotechnical Conf.* Richmond, BC.

Seed, H. B., and Idriss, I. M. (1982). "On the importance of dissipation effects in evaluating pore pressure changes due to cyclic loading." In *Soil mechanics—transient and cyclic loads*, 53-70.

Singh, S. (1994). "Liquefaction Characteristics of Silts." *Ground Failures under Seismic Conditions*, Geotech. Spec. Publ., 44, ASCE, New York, 105-116.

Stokoe, K. H., Roberts, J. N., Hwang, S., Cox, B. R., and Menq, F. (2016). "Effectiveness of inhibiting liquefaction triggering by shallow ground improvement methods: field shaking trials with T-Rex at one area in Christchurch, New Zealand." *24th Geotechnical Conference of Torino*, Turin, Italy.

Stokoe, K. H., and Santamarina, J. C. "Seismic-wave-based testing in geotechnical engineering." *Int. Conf. Geot. Geol. Eng., GeoEng 2000*, Melbourne, Australia, pp. 1490–1536.

Troncoso, J. H., and Verdugo, R. (1985). "Silt Content and Dynamic Behavior of Tailings Sands." *11th Int. Conf. Soil Mech. Fndn.Engrg.*, San Francisco, Vol. 3, pp.1311-1314.

Vaid, Y. P. (1994). "Liquefaction of Silty Soils." *Ground Failures under Seismic Conditions*, GSP No. 44, ASCE, 1-16.

Verma, P. (2019). *Monotonic and cyclic shear loading response of natural silts from british columbia, canada*. PhD dissertation., Dept. of Civil Engineering, University of British Columbia, Canada.

Vardanega, P. J., and Bolton, M. D. (2013). "Stiffness of clays and silts: Normalizing shear modulus and shear strain." *J. Geot. Geoenv. Eng.*, 139(9), 1575-1589.

Wijewickreme, D., Sriskandakumar, S., and Byrne, P. (2005). "Cyclic loading response of loose air-pluviated Fraser River sand for validation of numerical models simulating centrifuge tests." *Can. Geot. J.*, 42(2), 550-561.

Wijewickreme, D., and Sanin, M. (2010). "Postcyclic reconsolidation strains in low-plastic Fraser river silt due to dissipation of excess pore-water pressures." *J. Geot. Geoenv. Eng.*, 136(10), 1347-1357.

Wijewickreme, D., Soysa, A., and Verma, P. (2019). "Response of natural fine-grained soils for seismic design practice: A collection of research findings from British Columbia, Canada." *Soil Dyn. Earthq. Eng.*, 124, 280-296.